NIR-assisted orchid virus therapy using urchin bimetallic nanomaterials in phalaenopsis

2013 Adv. Nat. Sci: Nanosci. Nanotechnol. 4 045006

(http://iopscience.iop.org/2043-6262/4/4/045006)

OPEN ACCESS
IOP PUBLISHING
ADVANCES IN NATURAL SCIENCES: NANOSCIENCE AND NANOTECHNOLOGY
Adv. Nat. Sci.: Nanosci. Nanotechnol. **4** (2013) 045006 (6pp)
doi:10.1088/2043-6262/4/4/045006

NIR-assisted orchid virus therapy using urchin bimetallic nanomaterials in phalaenopsis

Shin-Yu Chen[1,6], Liang-Chien Cheng[2,6], Chieh-Wei Chen[2], Po-Han Lee[2], Fengjiao Yu[3], Wuzong Zhou[3], Ru-Shi Liu[2,4], Yi-Yin Do[1] and Pung-Ling Huang[1,5]

[1] Department of Horticulture and Landscape Architecture, National Taiwan University, Taipei 10617, Taiwan
[2] Department of Chemistry, National Taiwan University, Taipei 10617 , Taiwan
[3] Department of Chemistry, University of St Andrews, St Andrew, UK
[4] Genomics Research Center, Academia Sinica, Taipei 115, Taiwan
[5] Graduate Institute of Biotechnology, Chinese Culture University, No. 55, Hwa-Kang Road, Yang Ming Shan, Taipei 11114, Taiwan
[6] These authors contributed equally to this work.

E-mail: rsliu@ntu.edu.tw, yiyindo@ntu.edu.tw and pungling@ntu.edu.tw

Received 22 June 2013
Accepted for publication 11 July 2013
Published 14 August 2013
Online at stacks.iop.org/ANSN/4/045006

Abstract
The use of nanoparticles has drawn special attention, particularly in the treatment of plant diseases. Cymbidium mosaic virus (CymMV) and *Odontoglossum* ring spot virus (ORSV) are the most prevalent and serious diseases that affect the development of the orchid industry. In this study we treated nanoparticles as a strategy for enhancing the resistance of orchids against CymMV and ORSV. After chitosan-modified gold nanoparticles (Au NPs) were injected into *Phalaenopsis* leaves, the injected leaves were exposed to 980 nm laser for light–heat conversion. To evaluate virus elimination in the treated *Phalaenopsis* leaves, the transcripts of coat protein genes and the production of viral proteins were assessed by reverse transcription-Polymerase chain reaction and enzyme-linked immunosorbent assay, respectively. The expression of coat protein genes for both CymMV and ORSV was significantly lower in the chitosan-modified Au NP-treated *Phalaenopsis* leaves than in the control. Similarly, the amount of coat proteins for both viruses in the *Phalaenopsis* leaves was lower than that in the control (without nanoparticle injection). We propose that the temperature increase in the chitosan-modified Au NP-treated *Phalaenopsis* tissues after laser exposure reduces the viral population, consequently conferring resistance against CymMV and ORSV. Our findings suggest that the application of chitosan-modified Au NPs is a promising new strategy for orchid virus therapy.

Keywords: cymbidium mosaic virus, odontoglossum ring spot virus, gold, nanoparticles, photothermal therapy
Classification numbers: 2.04, 4.02, 5.08

1. Introduction

Orchidaceae is one of the largest families of angiosperms, comprising approximately 20 000–25 000 species. Orchid flowers are morphologically diverse, as in the patterns of colors in sepals, petals and lips. In addition, the column helps facilitate pollination [1]. The genus *Phalaenopsis* is a popular pot plant with high economic value in the flower market worldwide because of its graceful appearance, long flowering age and wide variety of species.

Cymbidium mosaic virus (CymMV) and odontoglossum ring spot virus (ORSV) are the most prevalent and serious

diseases that affect the development of the orchid industry [2]. As indicated by statistical data, CymMV and ORSV infect at least 80% of all virus-infected orchids [3]. The variability in coat protein gene sequences of CymMV and ORSV are highly conserved, enabling these two viruses to naturally infect orchids worldwide [4]. CymMV and ORSV reduce yield and diminish the quality of orchid flowers and plant vigor, thereby affecting the economic value of orchids. CymMV induces floral and foliar necrosis and ORSV causes ring spots on leaves. Although the plant exhibits symptoms, such as color breakage in flowers, blossom brown necrotic streaks may possibly result from mixed infection by CymMV and ORSV [5]. These two viruses mostly infect cultivated orchids but very few wild orchids [2]. Nevertheless, no effective method for protecting orchid plants from viral diseases has been developed.

To date, the most popular method is to use plant genetic transformation to solve the disease problem, but this approach presents certain disadvantages: it is time consuming, costly and involves lengthy culture procedures to produce stable transgenic plants. Nanoparticles have recently been extensively applied in plants. For example, researchers have delivered nanoparticles into plant tissues, with the materials remaining stable in plant cell or tissue [6–8]. Despite this progress, limited studies have been devoted to crop production or quality improvement by nanoparticle application. No clear direction has emerged as to establishing a direct relationship between plant disease and nanoparticle function.

Nanomaterials have been widely investigated in many fields, including energy and biology [9–11]. Investigations on bio-application, however, focus on animals. Given this backdrop, we used nanoparticles in CymMV and ORSV as two types of orchid virus therapy in *Phalaenopsis*. To the best of our knowledge, this study is the first to attempt the use of gold nanoparticle (Au NP) injection for application in orchid virus therapy. This study provides a fast and convenient method for enhancing disease resistance in orchids.

2. Experimental

2.1. Synthesis of urchin-like Au/Ag nanomaterials

The synthesis route of urchin-like Au/Ag bimetallic nanomaterials was presented elsewhere [12]. In brief, the nanomaterials were fabricated by mixing 20 μl 10 mM chloroauric acid ($HAuCl_4$), 2 μl 10 mM aqueous silver nitrate ($AgNO_3$), and 1 ml milli-Q deionized water in a 2 ml centrifugal tube. Then, 4 μl of 100 mM ascorbic acid (AA) was quickly added to the mixture, and vigorously shaken for 20 s. The mixture instantly changed from a light yellowish solution into a bluish solution, implying the fabrication of urchin-like Au/Ag nanomaterials by reduction. After a 1 min reaction, 1 wt% aqueous *O*-carboxymethylchitosan or fluorescein isothiocyanate (FITC)-capped *O*-carboxymethylchitosan was chosen as surfactant and added into the solution for reacting one more day. The mixture was centrifuged at 9279 *g* three times and redispersed into deionized water for further investigation. The morphologies of urchin-like Au/Ag nanomaterials can be altered by tuning metal precursors.

2.2. Plant materials and growth conditions

Phalaenopsis 'Sogo Yukidian' was used in the analysis of near-infrared light (NIR)-assisted virus therapy. The plants were kept in a greenhouse with natural light and a controlled temperature of 27/22 °C (day/night). They were checked for the absence of two prevalent orchid viruses, CymMV and ORSV by detecting the coat protein through enzyme-linked immunoassay (ELISA) before experimentation.

2.3. Virus inoculation and nanoparticle injection

The virus-free *Phalaenopsis* plants were inoculated by agroinfiltration of *Agrobacterium tumefaciens* containing CymMV or ORSV viral vector before the nanoparticle injection experiment. *Agrobacterium* was grown overnight at 28 °C and diluted to optical density at 600 nm (OD_{600}) = 0.5 with an infiltration buffer (0.5% D-glucose, 50 mM MES, 2 mM $Na_3PO_4 \cdot 12H_2O$, and 100 μM acetosyringone) [13]. Successful systemic infection with the virus was confirmed by ELISA [14]. For leaf injection, nanoparticles were injected into the leaf surface with a 1 ml syringe in all treatments. After 1 day, the targeted leaf was irradiated using a 980 nm laser and collected 1, 3 and 7 days after treatment. The treated materials were frozen in liquid nitrogen and stored at 80 °C for future investigation.

2.4. Collection and processing of samples for microscopy analysis

Approximately 1 mm thick, hand-cut cross-sections of the samples were collected 48 and 72 h after application of FITC-labeled nanoparticles. Then, the cross-sections were observed under a microscope (Leica MZ FL-III). The images of the sections were taken with a Zeiss AxioCam MRc monochrome cooled-CCD camera. Transmission electron microscopic (TEM) and high resolution TEM (HRTEM) images were recorded on a Jeol JEM-2010 electron microscope operating at 200 kV

2.5. Quantitative reverse transcription polymerase chain reaction (RT-PCR)

Total ribonucleic acid (RNA) was extracted from the dissected leaves by using a MaestroZol™ RNA PLUS Extraction Reagent (Omics Biotechnology), and treated with RNase-free DNase (Stratagene) to remove residual DNA. For quantitative RT-PCR, the RNA template was mixed with KAPA SYBR Fast One-step qRT-PCR Kit (ABI Prism, KAPA Biosystem) on a Biometra RT-PCR system (TAIGEN Bioscience Corporation, Taiwan). The primers for CymMV coat protein gene were as follows: 5′-TACTACGCAAAAGTGGTGTGGAAT-3′ as forward primer and 5′-AGAGCATAGAGAGTGTTGGTGGAG-3′ as reverse primer. The ORSV coat protein gene was amplified using 5′-AATCAACCTTTGTACCAATTCTCTG-3′ as forward primer and 5′-AGACTTGATTGTACGTACCAG TTCC-3′ as reverse primer. The housekeeping gene actin (PACT4, AY134752) was amplified using 5′-GCTGGCATATATTGCTCTTGATTAT-3′ as forward primer and 5′-ATCCAAACACTGTACTTCCTCTCTG-3′ as

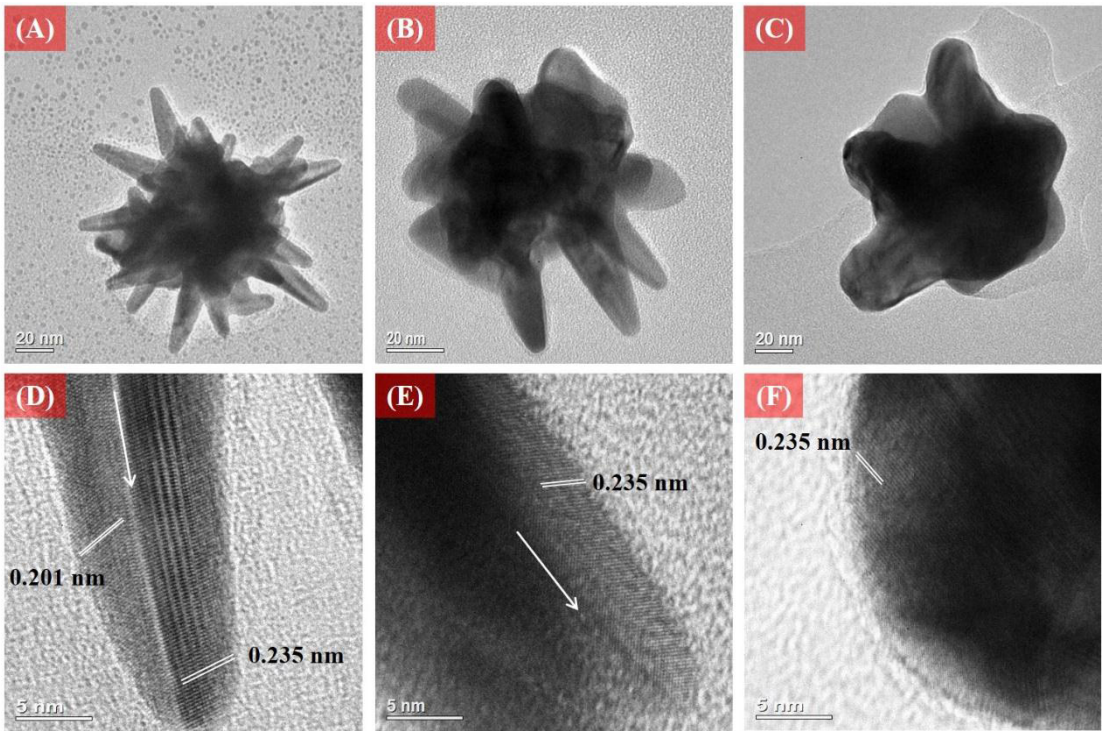

Figure 1. TEM (A,B,C) and HRTEM (D,E,F) bright field images of Au/Ag nanocrystals synthesized with various Au/Ag ratios; (A, D) 10, (B, E) 25 and (C, F) 100. The arrows show the growth direction of the thorns.

reverse primer used for data normalization. The PCR reaction conditions were 42 °C for 5 min, then 95 °C for 5 min, and thermal cycling for 40 cycles (95 °C for 3 s and 60 °C for 30 s). The relative quantification was calculated according to the manufacturer's protocols.

2.6. Quantification of coat protein by ELISA

The *Phalaenopsis* leaves (1 g) were homogenized by grinding in a mortar and pestle in 3 ml extraction buffer (100 mM Tris-HCl, pH 8.0, 10 mM KCl, 1 mM ethylenediaminetetraacetic acid (EDTA), 30 mM sodium ascorbate, 0.7% 2-mercaptoethanol, 5 mM dithiothreitol and 2 mM phenylmethylsulfonyl fluoride); the total soluble proteins were then extracted as previously described [14]. The leaf homogenate contained approximately 1.0–1.2 mg of total soluble protein as determined by a Protein Assay Kit (Bio-Rad). The total soluble protein was used to coat the ELISA plate (PerkinElmer) at 10 μg per well in 50 μl of coating buffer (1.59 g l^{-1} Na_2CO_3, 2.93 g l^{-1} $NaHCO_3$, 0.2 g l^{-1} NaN_3, pH 9.6), and the expression levels of coat protein were measured by ELISA. The ELISA plates were placed at 37 °C overnight, and then washed three times with phosphate buffered saline (PBS) containing 0.05% Tween-20 (Sigma) (PBST). After being washed with PBST, the wells were loaded with 1:1000 diluted rabbit anti-CymMV or anti-ORSV monoclonal antibody at 50 μl per well and incubated at 37 °C for 2 h. The wells were then washed three times with PBST, and loaded with 1:1000 diluted anti-rabbit Immunoglobulin G (IgG) and ABC Kit (Vector Laboratories Inc.). The wells were incubated at 37 °C for 2 h, followed by three washes with PBST. The plates were then developed with ρ-nitrophenylphosphate substrates and detected on an ELISA reader (Thermo) at 405 nm.

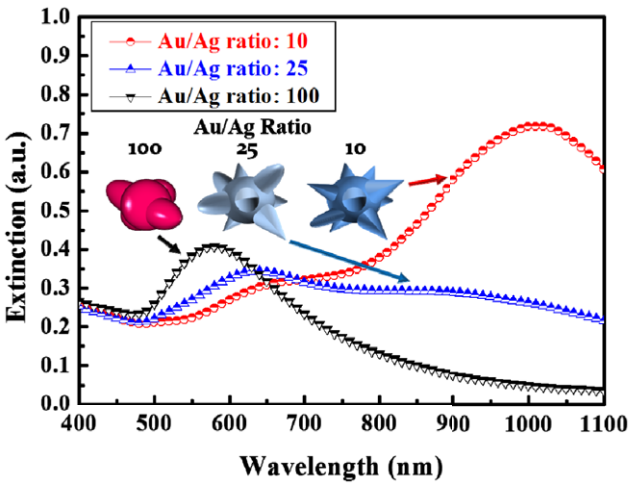

Figure 2. Corresponding extinction of various Au/Ag NPs.

3. Results and discussion

3.1. Synthesis and characterization of urchin-like nanomaterials

To fabricate urchin-like gold/silver bimetallic nanoparticles, the metal precursors $HAuCl_4$ and $AgNO_3$ were first mixed in aqueous solution at room temperature. An appropriate amount of aqueous AA solution was added into the mixed solution to fabricate diverse gold/silver bimetallic nanoparticles. Urchin-like, popcorn-like or irregularly spherical bimetallic nanoparticles were obtained in 1 min as varied by the mixed ratio of $HAuCl_4/AgNO_3$ (Au/Ag). In the reaction, the pH value was kept in an acidic condition (i.e. 3.0–3.4) for the growth of asymmetrical nanoparticles. The bio-friendly

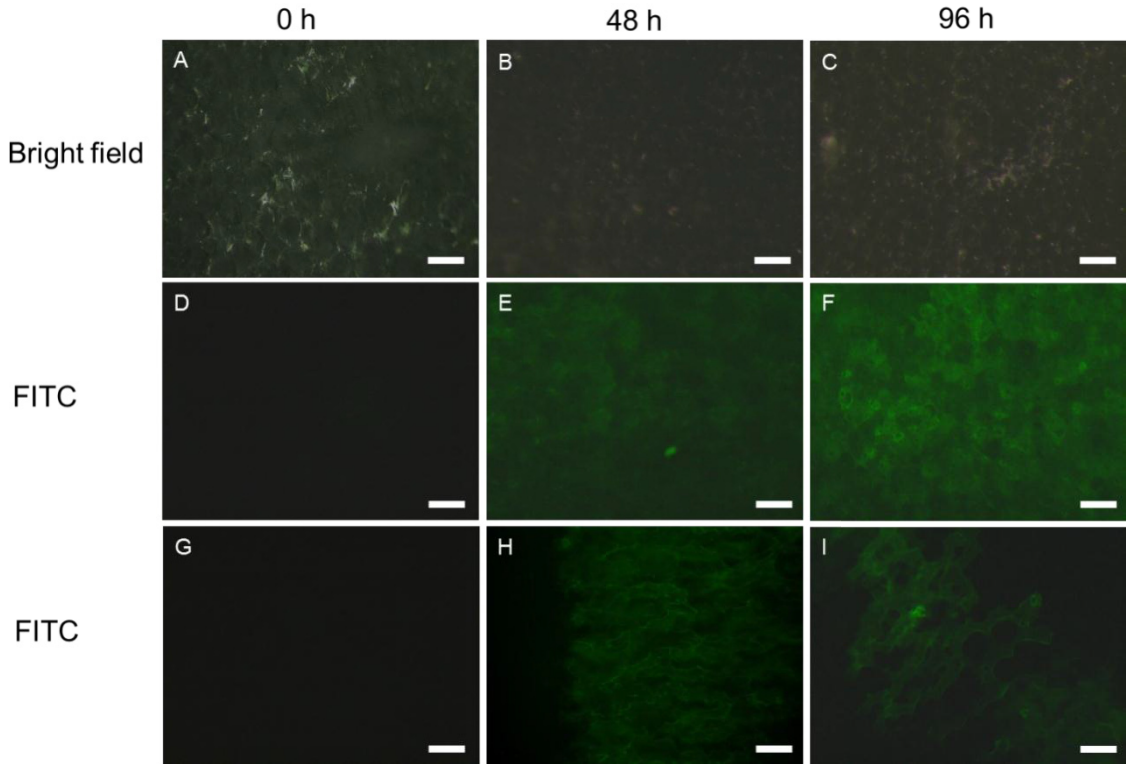

Figure 3. Microscopic examination of *Phalaenopsis* leaves injected with chitosan-modified Au NPs. Free-hand cross-section of leaves under bright field (A–C) and FITC fluorescence (D–I). Bars = 50 μm in (A–F) and bars = 150 μm in (G–I).

stabilizer, 1 wt% aqueous *O*-carboxymethylchitosan solution, was added into the solution.

Figure 1(A) shows the spiky urchin-like gold/silver bimetallic nanoparticles. As the proportion of gold ions increases, the thorns become fewer and larger. Figures 1(B) and (C) reveal that the morphologies of the nanoparticles become popcorn-like or irregular cores without apparent thorns when the metal precursor Au/Ag ratios increase to 25 or 100. We attribute the mechanism to the deposition of silver atoms on the surface of the pre-formed gold spherical nanostructures, which act as active sites for further growth of the thorns [12]. The calculation of the *d*-spacings in the HRTEM images shows that the nanoscale thorns grow along the [112] direction, which might be a consequence of a fast growth, i.e. controlled by kinetics, as being often observed in Si nanowires [15]. Figure 1(D) presents a typical single thorn. The crystal contains a large number of stacking-fault defects. The measured *d*-spacings of 0.235 and 0.201 nm are corresponding to the (111) and (200) planes of the face-centered cubic unit cell. Upon increasing the gold proportion, the urchin-like structure evolves into a popcorn-like structure with relatively smaller numbers and shorter thorns. Figure 1(E) shows an HRTEM image of a thorn from an urchin-like nanoparticle, showing a similar microstructure. Irregular bimetallic nanoparticles were obtained with an increase in Au/Ag ratio to 100. Figure 1(F) reveals that the branches grow to a broader form than those obtained in previous syntheses, and develop as quasi-spherical shapes instead of sharp-tip structures. Many domains can be observed and their crystal orientations are quite random. Moreover, the surface amorphous layers of the nanoparticles as seen in the HRTEM image in figure 1(F) show that the stabilizer molecules, *O*-carboxymethylchitosan, envelope the nanoparticles and maintain the morphologies or physical properties of the nanomaterials. Thus, the precursor ratio of Au/Ag significantly affects the morphology of the nanoparticles, which in turn changes the corresponding surface plasmon resonance.

The morphology of metal nanoparticles strongly influences their corresponding extinction wavelength because of changes in surface plasmon resonance. In figure 2, the extinction spectra show that as the aspect ratio of the tips decreases, the surface plasmon resonance bands blue shift from the near infrared to the visible range. The urchin-like Au/Ag NPs, which were produced at an Au/Ag ratio of 10, provide a major 1000 nm near-infrared longitudinal band and a minor 700 nm red light transverse band because of the large aspect ratio of the tips. With the morphology of the nanoparticles changing from an urchin-like to popcorn-like or spherical morphology, the extinction also changes to major visible light because of the decreasing aspect ratio of the nanoparticles. According to previous studies, the Au/Ag NPs present a high light–heat transformation, providing strong local heat after specific surface plasmon band irradiation. The urchin-like Au/Ag NPs were selected as a candidate as photothermal reagents because of their strong near-infrared absorbance, which enables deeper penetration into tissues than that achieved with visible or ultraviolet light.

3.2. Identification of fluorescein isothiocyanate-labeled nanoparticles in plant tissue

Viral diseases affecting orchid flower quality is a critical dilemma in the global orchid industry. No effective solution

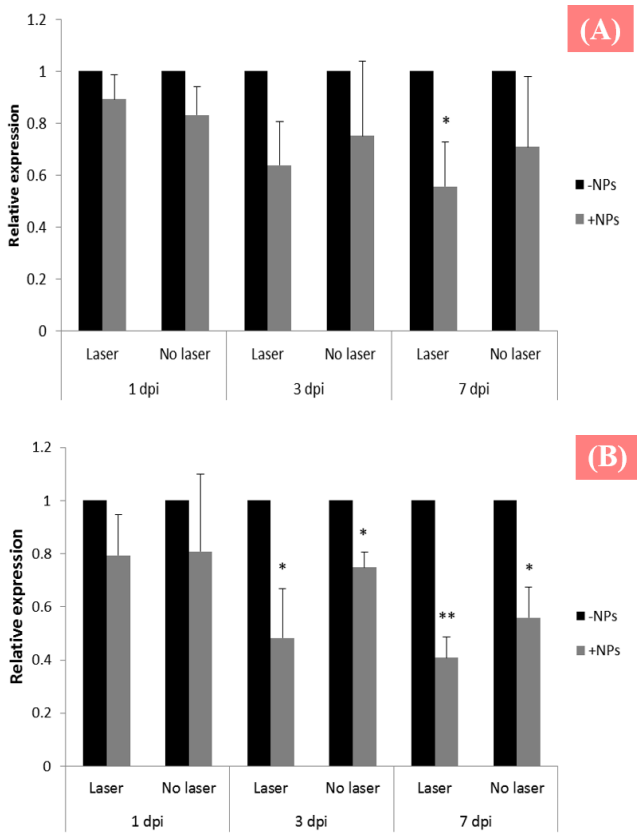

Figure 4. Relative expression of coat protein gene of CymMV (A) and ORSV (B) in *Phalaenopsis* leaves by RT-PCR. *Phalaenopsis* leaves were inoculated first with CymMV or ORSV alone. Injection of infected leaves with or without chitosan-modified Au NPs was conducted 7 days after inoculation. Laser exposure was performed immediately after injection. Samples were collected at 1, 3 and 7 days after injection (dpi) and compared to the untreated samples. All data represent the average values of three replicates. Presented data were normalized to without chitosan-modified Au NP injection.$^{*}P < 0.05$, $^{**}P < 0.01$ (*t*-test), indicating a significant difference between the leaves injected with or without chitosan-modified Au NPs. Error bars show standard deviations.

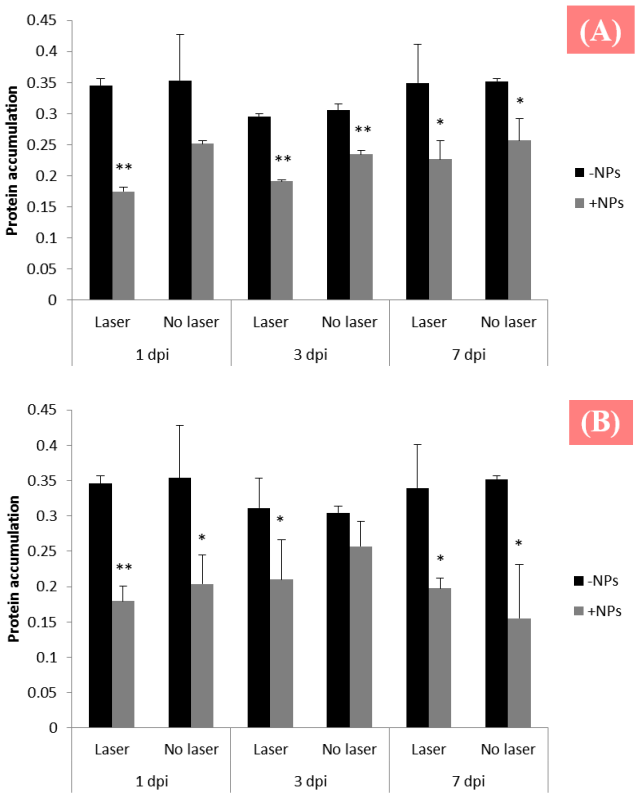

Figure 5. Coat protein accumulation of CymMV (A) and ORSV (B) as determined by ELISA. *Phalaenopsis* leaves were inoculated first with CymMV or ORSV alone. Injection of infected leaves with or without chitosan-modified Au NPs was conducted 7 days after inoculation. Laser exposure was performed immediately after injection. Samples were collected at 1, 3 and 7 days after injection (dpi) and compared with untreated samples. Measurements were done by ELISA analysis with absorbance recorded at 405 nm after 30 min of incubation with the substrate. All data represent the average values of three replicates. $^{*}P < 0.05$, $^{**}P < 0.01$ (*t*-test), indicating a significant difference between the leaves injected with or without chitosan-modified AU NPs. Error bars show standard deviations.

has been developed for this problem. Although the application of nanotechnology to biology has mostly focused on animal and medical research, we demonstrate a nanomaterial that may be applied in plant science research and in the improvement of crop production. Accordingly, we developed a technical approach for the agricultural application of nanoparticles. In previous research, a mesoporous silica nanoparticle system was developed that can transport DNA and chemicals into tobacco protoplast and the intact leaves of young maize embryos [8]. Corredor *et al* [6] indicated that nanoparticles can penetrate living pumpkin plant tissue and migrate to different regions of the plant. Thus, further directed delivery of substances into plant cells is a feasible application. In the present study we also demonstrated that nanoparticles can penetrate *Phalaenopsis* leaf tissue and migrate to different regions of the plant (figure 3).

To test nanoparticle penetration, labeling with FITC was carried out. Fluorescence microscopy analysis shows that without injection, protoplasts do not exhibit fluorescence in the FITC-specific filter set (figures 3(A), (D), (G)). By contrast, after 48 and 96 h, fluorescence occurs under FITC fluorescence. The fluorescence is expressed in the intercellular spaces of the tissue (figures 3(E) and (F)), indicating that FITC-labeled nanoparticles are present in the plant. The magnified image at the bottom of figures 3(G) and (I) show the same results. The penetration of nanomaterials into tissue can shorten the distance between viral tissue targeting and nanomaterials for enhancing therapeutic efficiency.

3.3. Photo-induced virus elimination by injection of urchin-like nanomaterials

To investigate whether nanoparticles diminish virus density, we injected the nanoparticles into the infected *Phalaenopsis* leaves, and collected the leaves 1, 3 and 7 days after injection. RT-PCR was performed to confirm the expression of CymMV or ORSV coat protein gene. The results show that CymMV coat protein gene expression decreases immediately after injection with the nanoparticles. CymMV transcripts decrease in comparison with the control (injected with sterile distilled water), and messenger RNA (mRNA) expression slightly decreases with laser treatment (figure 4(A)). ORSV coat protein gene expression also shows a decreasing trend in the expression pattern, depending on the time of inoculation,

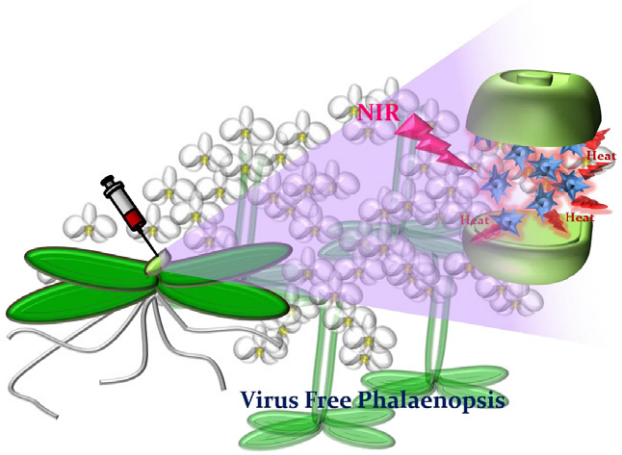

Figure 6. Pictured presentation content. Urchin-like nanomaterials can convert light into heat via NIR irradiation and eliminate the cymbidium mosaic virus and *Odontoglossum* ring spot virus in *Phalaenopsis*.

and expression decreases in comparison with the control (injected with sterile distilled water) (figure 4(B)). The results reveal that laser is significantly related to decreased CymMV or ORSV gene expression and protein accumulation by enhancing the effect of nanoparticles. As treatment progressed, however, the transcript level of CymMV and ORSV transcripts gradually decreases. Consistent with this result, CymMV and ORSV coat proteins were also detected by ELISA. We found that in the plant injected with the nanoparticles, CymMV and ORSV coat protein accumulation levels are lower than that in the control. mRNA expression slightly decreases with laser treatment (figure 5).

We found that CymMV and ORSV expression decreases two- to three-fold, and protein accumulation decreases one- to two-fold, suggesting that nanoparticle injection with laser treatment effectively reduces CymMV and ORSV coat protein gene expression and protein accumulation (figures 4 and 5). Chitosan, which was selected as nanoparticle stabilizer, may inhibit virus growth. Hirano [16] pointed out that chitinase isoforms are one group of pathogenesis-related proteins in plants. As a chitinase isoform, chitosan may be used to promote tissue growth and differentiation in tissue culture, as well as to induce plant defense. Moreover, virus reduction may be attributed to the ability of nanoparticles to convert absorbed near-infrared irradiation into heat (figure 6). Local temperature increases, thereby preventing virus differentiation and directly eliminating the virus. As presented in the results, photo-induced virus elimination efficiently enhances therapeutic behavior. In the future, nanomaterials may be conjugated with specific proteins to target CymMV and ORSV for a more highly efficient treatment system.

4. Conclusion

We have demonstrated that urchin-like Au/Ag bimetallic nanoparticles can enter virus tissue via injection. Intercellular nanoparticles may decrease the gap between targeting virus tissue and enhancing therapeutic behavior. Moreover, injected nanomaterials can kill viruses and increase resistance of plants against orchid viruses; this approach is therefore a convenient method for conferring resistance to orchids against CymMV and ORSV. Finally, this study can be a particularly essential reference for future research and lead to a better understanding of the application of nanoparticles in enhancing virus resistance in plants.

Acknowledgments

The authors would like to thank the Council of Agriculture (grant number 101AS-9.1.1-FD-Z1) of Taiwan and National Science Council (contracts numbers NSC 101-2113-M-002-014-MY3 and NSC 101-3113-P-002-021) for financially supporting this research.

References

[1] Yu H and Goh C J 2001 *Plant Physiol.* **127** 1390
[2] Zettler F W, Ko N J, Wisler G C, Elliott M S and Wong S M 1990 *Plant Dis.* **74** 621
[3] Wong S M, Chng C G, Lee Y H, Tan K and Zettler F W 1994 *Crop. Prot.* **13** 235
[4] Ajjikuttira P A, Lim-Ho C L, Woon M H, Ryu K H, Chang C A, Loh C S and Wong S M 2002 *Arch. Virol.* **147** 1943
[5] Hu J S, Ferreira S, Wang M and Xu M Q 1993 *Plant Dis.* **77** 464
[6] Corredor E *et al* 2009 *BMC Plant Biol.* **9** 1
[7] Gonzalez-Melendi P, Fernandez-Pacheco R, Coronado M J, Corredor E, Testillano P S, Risueno M C, Marquina C, Ibarra M R, Rubiales D and Perez-De-Luque A 2008 *Ann. Bot.* **101** 187
[8] Torney F, Trewyn B G, Lin V S Y and Wang K 2007 *Nature Nanotechnol.* **2** 295
[9] Chen H M *et al* 2012 *ACS Nano* **6** 7362
[10] Cheng L C, Chen H M, Lai T C, Chan Y C, Liu R S, Sung J C, Hsiao M, Chen C H, Her L J and Tsai D P 2013 *Nanoscale* **5** 3931
[11] Cheng L C, Jiang X M, Wang J, Chen C Y and Liu R S 2013 *Nanoscale* **5** 3547
[12] Cheng L C, Huang J H, Chen H M, Lai T C, Yang K Y, Liu R S, Hsiao M, Chen C H, Her L J and Tsai D P 2012 *J. Mater. Chem.* **22** 2244
[13] Sparkes I A, Runions J, Kearns A and Hawes C 2006 *Nature Protocol.* **1** 2019
[14] Arakawa T, Chong D K X, Merritt J L and Langridge W H R 1997 *Transgenic Res.* **6** 403
[15] Su Z X, Dickinson C, Wan Y T, Wang Z L, Wang Y W, Sha J and Zhou W Z 2010 *Cryst. Eng. Commun.* **12** 2793
[16] Hirano S 1999 *Polym. Int.* **48** 732